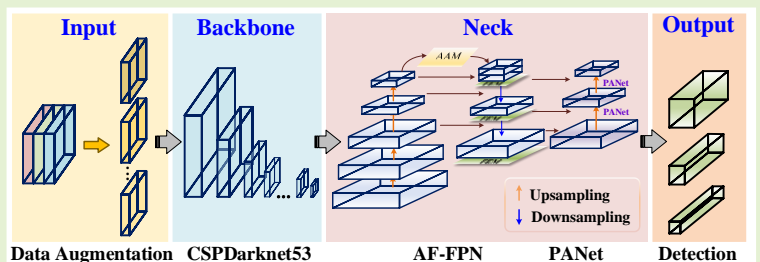


Improved YOLOv5 network for real-time multi-scale traffic sign detection

Junfan Wang, Yi Chen, Mingyu Gao, and Zhekang Dong, *Member IEEE*

Abstract—Traffic sign detection is a challenging task for the unmanned driving system, especially for the detection of multi-scale targets and the real-time problem of detection. In the traffic sign detection process, the scale of the targets changes greatly, which will have a certain impact on the detection accuracy. Feature pyramid is widely used to solve this problem but it might break the feature consistency across different scales of traffic signs. Moreover, in practical application, it is difficult for common methods to improve the detection accuracy of multi-scale traffic signs while ensuring real-time detection. In this paper, we propose an improved feature pyramid model, named AF-FPN, which utilizes the adaptive attention module (AAM) and feature enhancement module (FEM) to reduce the information loss in the process of feature map generation and enhance the representation ability of the feature pyramid. We replaced the original feature pyramid network in YOLOv5 with AF-FPN, which improves the detection performance for multi-scale targets of the YOLOv5 network under the premise of ensuring real-time detection. Furthermore, a new automatic learning data augmentation method is proposed to enrich the dataset and improve the robustness of the model to make it more suitable for practical scenarios. Extensive experimental results on the Tsinghua-Tencent 100K (TT100K) dataset demonstrate the effectiveness and superiority of the proposed method when compared with several state-of-the-art methods.

Index Terms—AF-FPN, data augmentation, multi-scale target, YOLOv5



I. INTRODUCTION

THE traffic sign recognition system is an important part of the ITS and unmanned driving system. How to improve the accuracy and real-time performance of the traffic sign detection and recognition technology, which is the key problem that needs to be solved when the technology moves toward the actual application [1].

In recent years, most of the state-of-the-art object-detection algorithms, such as Faster R-CNN [2], R-FCN [3], SSD [4], and YOLO [5], have used convolutional neural networks (CNNs) and achieved fruitful achievements in object detection tasks. However, simply applying these methods to traffic sign

recognition is hard to get a satisfactory performance. The target recognition and detection of the vehicle-mounted mobile terminal require high accuracy for targets of different scales, and high requirements for recognition speed, which means to meet the two requirements of accuracy and real-time [6, 7].

Traditional CNNs usually need a large number of parameters and floating-point operations (FLOPs) to achieve a satisfactory accuracy, *e.g.* ResNet-50 [8] has about 25.6M parameters and requires 4.1B FLOPs to process an image of size 224×224 . However, mobile devices (*e.g.* smartphones and self-driving cars) with limited memory and computation resources cannot be used for deployment and inference for larger networks. As a one-stage detector, the YOLOv5 [9] is used in this paper because of the advantages of low computation and fast recognition speed.

In this paper, an improved YOLOv5 network is proposed, which not only ensures that the model size can meet the requirements of deployment on the vehicle side but also improve the ability of multi-scale targets and meet the real-time requirement.

The main contributions of our work are summarized as follows:

- 1) A novel feature pyramid network is proposed in this paper. Through adaptive feature fusion and receptive field enhancement, it retains the channel information in the feature transfer process to a large extent and learns different receptive fields in each feature map adaptively to enhance the representations of feature pyramids, effectively improving the accuracy of multi-scale targets recognition.

This work was supported in part by the National Natural Science Foundation of China under Grant 61873077; in part by the Key Research and Development Program of Zhejiang Province under Grant 2020C01110. The associate editor coordinating the review of this article and approving it for publication was Prof. Mingyu Gao. (*Corresponding author: Mingyu Gao*)

Junfan Wang and Yi Chen are with the College of Electronic Information, Hangzhou Dianzi University, Hangzhou 310018, China. (e-mail: wangjunfan@hdu.edu.cn; chenyi2026@hdu.edu.cn).

Mingyu Gao is with the Zhejiang Provincial Key Lab of Equipment Electronics, Hangzhou 310018, China, and also with the College of Electronic Information, Hangzhou Dianzi University, Hangzhou 310018, China. (e-mail: mackgao@hdu.edu.cn).

Zhekang Dong is with Department of Electrical Engineering, Zhejiang University, Hangzhou 310027, China, and also with the College of Electronic Information, Hangzhou Dianzi University, Hangzhou 310018, China. (e-mail: englishp@126.com).

2) A new automatic learning data augmentation strategy is proposed. Inspired by AutoAugment [10], the latest data augmentation operations have been added. The improved data augmentation method effectively improves the model training effect and the robustness of the training model, which has more practical significance.

3) Unlike the existing YOLOv5 network, the current version is improved to reduce the impact of scale invariance. Meanwhile, it can be deployed on the mobile terminal of the vehicle to detect and recognize traffic signs in real-time.

The rest of this paper is organized as follows: Section II introduces related works about CNN-based traffic sign detection and data augmentation. Section III introduces the details of the proposed method to detect and recognize the traffic signs efficiently in real-time. The experimental results and analysis are presented in Section IV. Finally, the conclusion is described in Section V.

II. RELATED WORKS

A. CNN-based traffic sign detection

At present, convolutional neural networks (CNNs) have achieved great success in visual object detection [11-14]. According to whether region proposal is needed, object detection based on deep learning can be divided into two categories: single-stage detection and two-stage detection.

Shao *et al.* [15, 16] proposed a regional suggestion algorithm to simplify the Gabor wavelet and improve Faster R-CNN to traffic sign detection. Zhang *et al.* [17] proposed an improved one-stage traffic sign detector based on YOLOv2, where they modified the number of convolutional layers in the classic YOLOv2 network to make it suitable for the China Traffic Sign Dataset. Li *et al.* [18] developed a novel perceptual generative adversarial network, which boosts detection performance by generating super-resolve representations for small traffic signs. SADANet [19] combines a domain adaptive network with a multi-scale prediction network to address scale variety problems.

Most of the above networks use the single-scale deep feature so it is difficult to improve the performance of detection and recognition in sophisticated scenes. Scale variety problem is a challenge in traffic sign detection and recognition because there are completely different visual features between large traffic signs instances and small ones. And for object detection, learning scale-invariant representation is critical for recognizing and localizing objects [20]. Current work handles this challenge mainly from two aspects, namely network architecture and data augmentation [21].

At present, multi-scale features are widely used in high-level object recognition to improve the recognition performance of multi-scale targets [22]. Feature Pyramid Network (FPN) [23] is a commonly used multilayer feature fusion method, which derives many networks with high detection accuracy using its multi-scale expression ability, such as Mask R-CNN [24] and RetinaNet [25]. It is worth noting that the feature maps will suffer from information loss due to the reduced feature channels and only contain some less relevant context information in the feature maps of other levels. Moreover, using FPN can cause the network to pay too much attention to the optimization of low-level features, and sometimes result in

a decrease in the detection accuracy of large-scale targets [22]. In response to this problem, a simple yet effective method named receptive field pyramid (RFP) [26] is proposed to enhance the representation ability of feature pyramids and drive the network to learn the optimal feature fusion pattern [14].

B. Data augmentation

Data augmentation has been widely utilized for network optimization and proven to be beneficial in vision tasks [2, 27, 28], which can improve the performance of CNN, prevent over-fitting [29], and is easy to implement [30].

Data augmentation approaches could be roughly divided into color operations (*e.g.*, brightness, contrast, and color casting) and geometric operations (*e.g.*, scaling, flipping, translation, and zoom) [31]. These augmentation operations artificially inflate the training dataset size by either data warping or oversampling. Lv *et al.* [32] proposed five data augmentation methods dedicated to face image, including landmark perturbation and four synthesis methods (hairstyles, glasses, poses, illuminations). Nair *et al.* [33] applied two forms of data augmentation to training data. One is random crop and horizontal reflections, while the other is altering the intensities of the RGB channels by applying PCA on color space. These frequently used methods just do simple transformations and cannot meet the requirements of complex situations. Dwivedi *et al.* [34] improved detection performance with the cut-and-paste strategy. Furthermore, InstaBoost [35] augments training images using annotated instance masks with a location probability map. YOLOv4 [13] and Stitcher [36] introduce mosaic inputs that contain rescaled sub-images, which are also used in YOLOv5. However, these data augmentation implementations are manually designed and the best augmentation strategies are dataset-specific.

To avoid the data-specific nature of data augmentation, recent work has focused on learning data augmentation strategies directly from the data itself. Tran *et al.* [37] generated augmented data, using the Bayesian approach, based on the distribution learned from the training set. Cubuk *et al.* [10] proposed a new way of data augmentation called AutoAugment to automatically search for improved data augmentation policies.

III. PROPOSED METHOD

A. The improved YOLOv5s network framework

As the latest model in the current YOLO series, the superior flexibility of YOLOv5 makes it convenient for rapid deployment on the vehicle hardware side [38]. YOLOv5 contains four models, namely YOLOv5s, YOLOv5m, YOLOv5l, and YOLOv5x. YOLOv5s is the smallest model of the YOLO series and is more suitable for deployment on a vehicle-mounted mobile hardware platform due to its memory size of 14.10M, but the recognition accuracy cannot meet the requirements of accurate and efficient recognition, especially for the recognition of small-scale targets.

The basic framework YOLOv5 can be divided into four parts: Input, Backbone, Neck, and Prediction [38]. The Input part enriches the dataset with mosaic data augmentation, which has low requirements for hardware devices and low computational cost. However, it will cause the original small targets in the

dataset to become smaller, resulting in the deterioration of the generalization performance of the model. The Backbone part is mainly composed of CSP modules, which perform feature extraction through the CSPDarknet53 [13]. FPN and Path Aggregation Network (PANet) [39] are used to aggregate the image feature at this stage in Neck. Finally, the network performs target prediction and output through the Prediction.

In this paper, the AF-FPN and the automatic learning data augmentation are introduced to solve the problem of incompatibility between model size and recognition accuracy,

and further improve the recognition performance of the model. The original FPN structure is replaced by AF-FPN to improve the ability to recognize multi-scale targets and make an effective trade-off between recognition speed and accuracy [26]. Moreover, we remove the mosaic augmentation in the original network and use the best data augmentation methods according to the automatic learning data augmentation policy to enrich the dataset and improve the training effect. The improved YOLOv5s network structure is shown in Fig. 1.

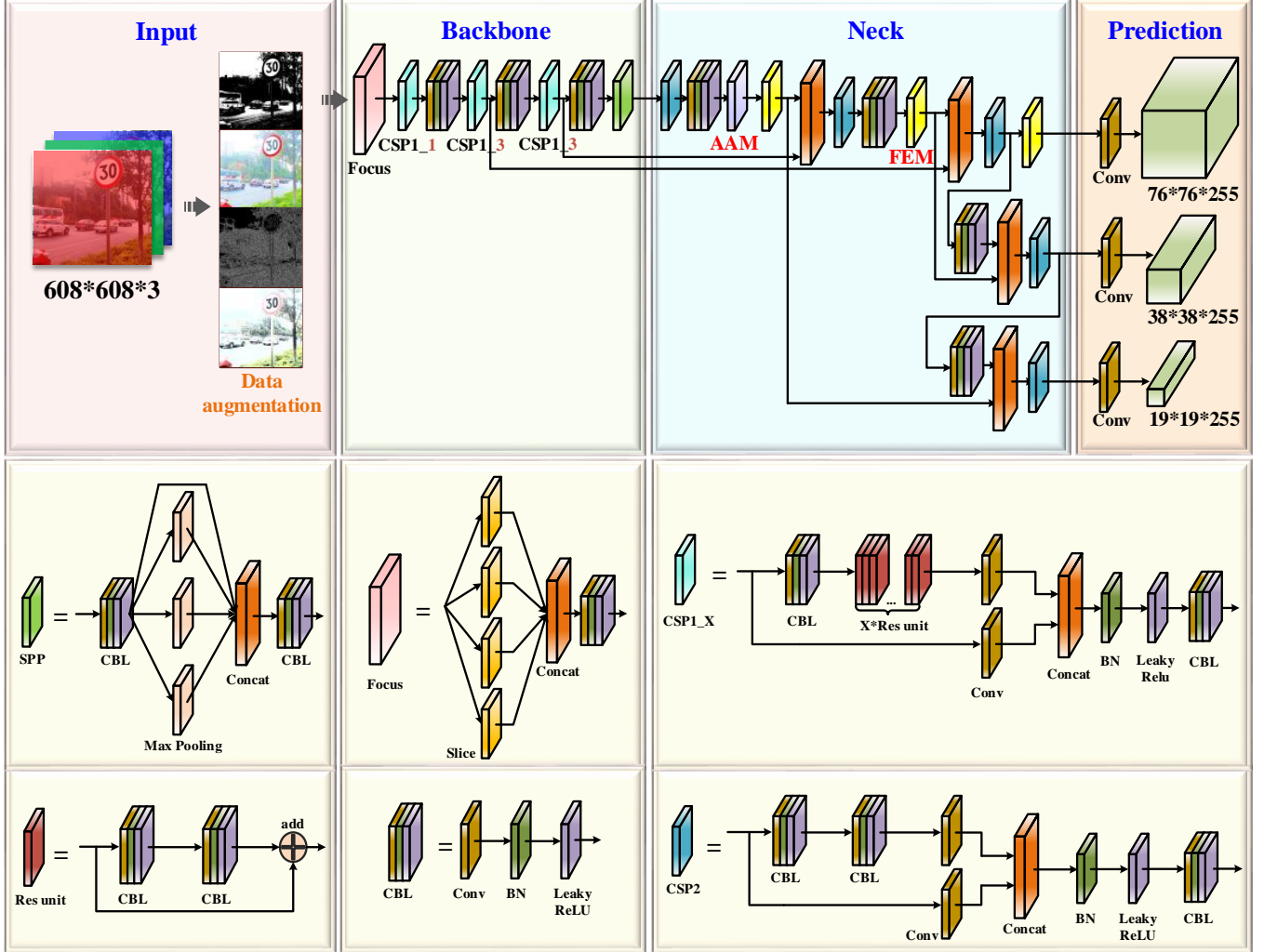


Fig. 1. The architecture of the proposed YOLOv5s network

In Prediction, generalized IoU (GIoU) [40] loss is used as the loss function of the bounding box and the weighted non-maximum suppression (NMS) [41] method is used for NMS. The loss function is as follows:

$$L_{GIoU} = 1 - IoU + \frac{|C - (B \cup B^{gt})|}{|C|} \quad (1)$$

$$IoU = \frac{|A \cap B|}{|A \cup B|} \quad (2)$$

where C is the smallest box covering B and B^{gt} . $B^{gt} = (x^{gt}, y^{gt}, w^{gt}, h^{gt})$ is the ground-truth box, and $B = (x, y, w, h)$ is the predicted box.

However, when the predicted box is inside the ground-truth box and the size of the predicted box is the same, the relative

positions of the predicted box and the ground-truth box cannot be distinguished.

In this paper, the GIoU is replaced by complete IoU (CIoU) [42] loss. Based on GIoU loss, the CIoU loss considers the overlap area, central point distance of bounding boxes, and the consistency of aspect ratios for bounding boxes. The loss function can be defined as:

$$R_{CIoU} = \frac{\rho^2(b, b^{gt})}{c^2} + \alpha v \quad (3)$$

$$v = \frac{4}{\pi^2} (\arctan \frac{w^{gt}}{h^{gt}} - \arctan \frac{w}{h})^2 \quad (4)$$

$$L_{CIoU} = 1 - IoU + R_{CIoU} \quad (5)$$

where R_{IoU} is the penalty term, which is defined by minimizing the normalized distance between central points of two bounding boxes. b and b^{gt} denote the central points of B and B^{gt} , $\rho(\cdot)$ is the Euclidean distance, and c is the diagonal length of the smallest enclosing box covering the two boxes. α is a positive trade-off parameter, and v measures the consistency of the aspect ratio.

And the trade-off parameter α is defined as

$$\alpha = \frac{v}{(1 - IoU) + v} \quad (6)$$

which the overlap area factor is given higher priority for regression, especially for non-overlapping cases.

B. AF-FPN structure

Based on the traditional feature pyramid network, AF-FPN adds the adaptive attention module (AAM) and the feature enhancement module (FEM). The former part reduces the loss of context information in the high-level feature map due to the reduced feature channels. The latter part enhances the representation of feature pyramids and accelerates the inference speed while achieving state-of-the-art performance. The structure of the AF-FPN is shown in Fig.2.

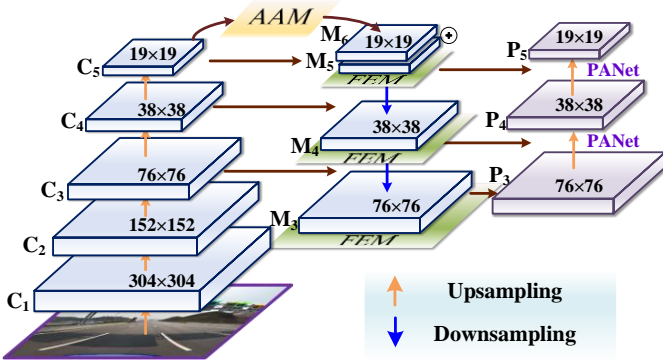


Fig. 2. The architecture of the AF-FPN.

The input image generates feature maps $\{C_1, C_2, C_3, C_4, C_5\}$ through multiple convolutions. C_5 generates the feature map M_6

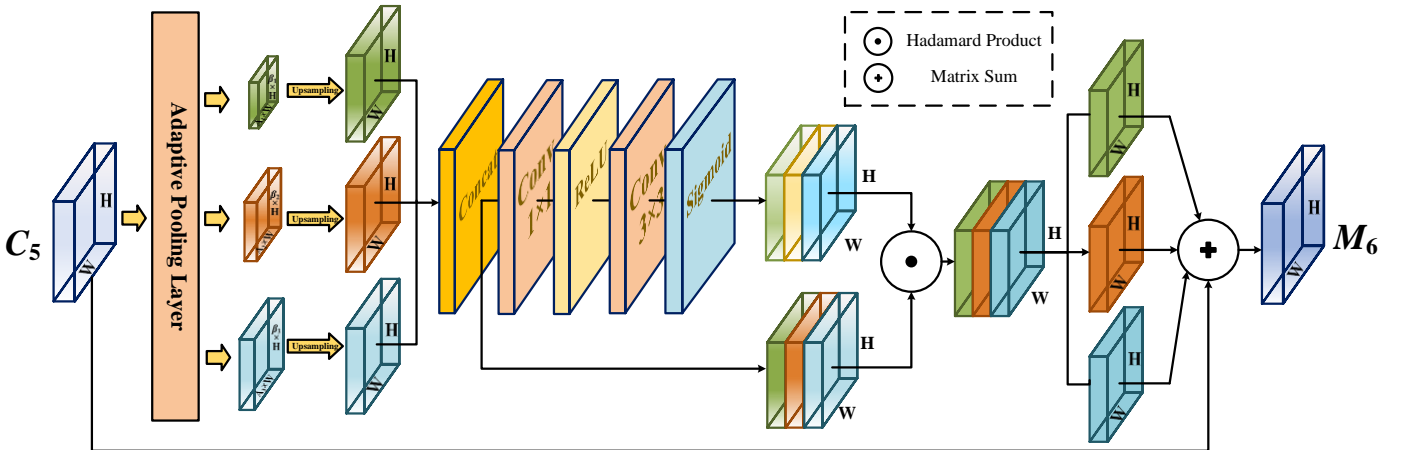


Fig. 3. The architecture of the AAM.

FEM mainly uses the dilated convolution to learn the different receptive fields in each feature map adaptively based on the varying scales of detected traffic signs, thereby improving the accuracy of multi-scale target detection and recognition. As shown in Fig.4, it can be divided into two

through AAM. And M_6 is combined with M_5 by summation and propagated to fuse with other features at lower levels through a top-down path, and the receptive field is expanded through FEM after each fusion. PANet shortens the information path between lower layers and the topmost feature.

The operation of the adaptive attention module can be performed in two steps. First of all, the multiple context features with different scales are obtained through the adaptive average pooling layer. The pooling coefficient β is $[0.1, 0.5]$, and it adaptively changes according to the target size in the dataset. Secondly, a spatial weight map is generated for each feature map through the spatial attention mechanism. Through the weight map, context features are fused to generate a new feature map, which contains multi-scale context information. The new feature map is combined with the original high-level feature map and propagated to fuse with other features at lower levels.

The specific structure of the AAM is shown in Fig. 3. As the input of the adaptive attention module, the size of C_5 is $S=h \times w$. It first obtains context features with different scales of $(\beta_1 \times S, \beta_2 \times S, \beta_3 \times S)$ through the adaptive pooling layer. Then each context feature undergoes a 1×1 convolution to obtain the same channel dimension 256. Bilinear interpolation is used to upsample them to the scale of S for subsequent fusion. The spatial attention mechanism merges the channels of the three context features through a Concat layer, and then the feature map sequentially passes 1×1 convolution layer, ReLU activation layer, 3×3 convolution layer, and sigmoid activation layer to generate corresponding spatial weights for each feature map. The generated weight map and the feature map after the merged channel are subjected to the Hadamard product operation, which is separated and added to the input feature map M_5 to aggregate context features into M_6 . The final feature map has rich multi-scale context information, which to a certain extent alleviates the loss of information due to the reduction of the number of channels.

components: the multi-branch convolution layer and the branch pooling layer. The multi-branch convolution layer is used to provide different sizes of receptive fields for the input feature map through the dilated convolution. And the average pooling layer is used to fuse the traffic information from the three

branch receptive fields to improve the accuracy of multi-scale prediction.

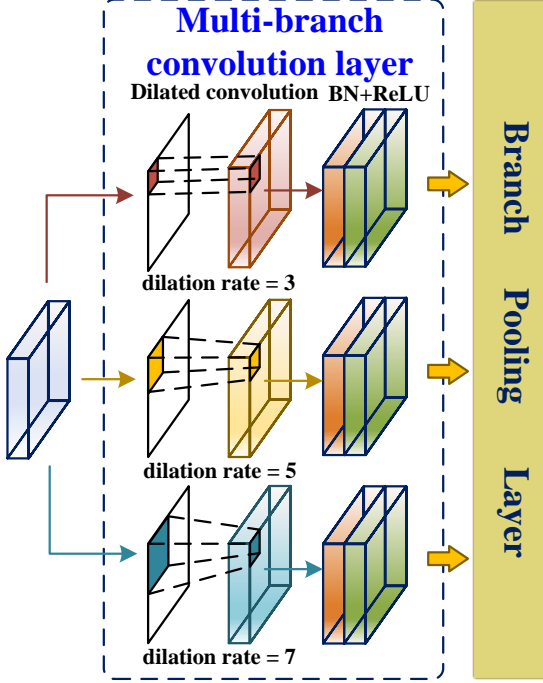


Fig. 4. The architecture of FEM

The multi-branch convolution layer consists of dilated convolution, BN layer, and ReLU activation layer. The dilated convolutions in the three parallel branches have the same kernel size but different dilation rates. Specifically, the kernel of each dilated convolution is 3×3 and the dilation rates d are 1, 3, and 5 for different branches.

Dilated convolutions support exponentially expanding receptive fields without losing resolution or coverage [43]. However, in the convolution operation of dilated convolution, the elements of the convolution kernel are spaced, and the size of the space depends on the dilation rates, which is different from the elements of the convolution kernel that are all adjacent in the standard convolution operation.

The convolution kernel changed from 3×3 to 7×7 and the receptive field of this layer is 7×7 . The formula for the receptive field of dilated convolution is as follows:

$$r_1 = d \times (k - 1) + 1 \quad (7)$$

$$r_n = d \times (k - 1) + r_{n-1} \quad (8)$$

where k and r_i denote the kernel size and dilation rate, respectively. And d denote the stride of the convolution.

The branch pooling layer [44] is proposed to fuse information from different parallel branches and avoid introducing additional parameters. The averaging operation is utilized to balance the representation of different parallels branches during training, which enables a single branch to implement inference during the test. The expression is as follows:

$$y_p = \frac{1}{B} \sum_{i=1}^B y_i \quad (9)$$

where y_p denotes the output of the branch pooling layer. B represents the number of parallel branches and we set $B = 3$.

C. Data Augmentation

The augmentation policy consists of two parts: search space and search algorithm [45]. In the search space, there are $S=5$ sub-policies with each sub-policy consisting of two image operations to be applied in sequence. One of the sub-policies are chosen at random and applied to the current image. In addition, each operation is also associated with two hyperparameters: the probability of applying the operation and the magnitude of the operation [10]. The operations we used in the experiment include the latest data augmentation methods such as Mosaic [13], SnapMix [46], Earsing, CutMix, Mixup and Translate X/Y. In total, we have 15 operations in our search space. Each operation also comes with a default range of magnitude. We discretize the range of magnitude into $D=11$ uniformly-spaced values so that we can use a discrete search algorithm to find them. Similarly, we also discretize the probability of applying an operation into $P=10$ values (uniform spacing). Finding each sub-policy becomes a search problem in a space of $(19 \times D \times P)^2$ possibilities. Therefore, the search space with 5 sub-policies then has roughly $(19 \times D \times P)^{2 \times 5}$ possibilities and requires an efficient search algorithm to navigate this space [47]. Fig. 5 shows the policy with 5 sub-policies in the search space.

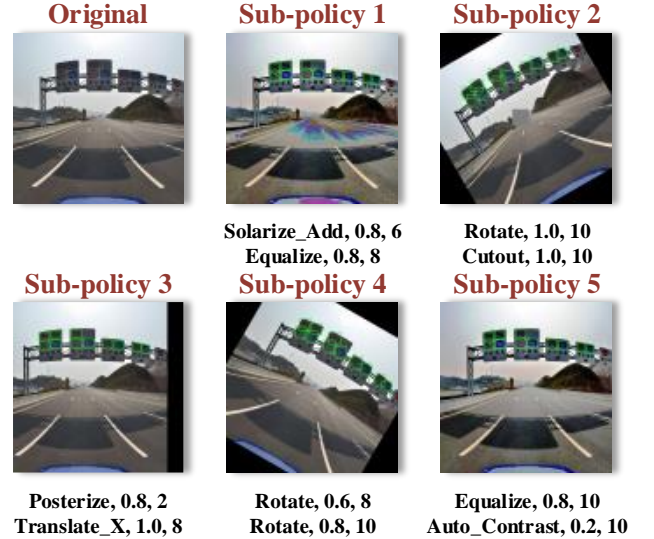


Fig. 5. An example of a policy with 5 sub-policies

Through the search space, the problem of searching for a learned augmentation policy into a discrete optimization problem. Reinforcement Learning [48] is used as the search algorithm, which has two components: a controller RNN and the training algorithm. The controller RNN is a recurrent neural network, and the training algorithm, which is the proximal policy optimization (PPO) [47] with a learning rate of 0.00035. The controller RNN predicts a decision produced by a softmax at each step and the prediction is then fed into the next step as an embedding from the search space. Totally, the controller has 30 softmax predictions to predict 5 sub-policies, each of which has two operations, and each operation requires an operation type, magnitude, and probability. We applied the automatic learning data augmentation method to the TT100K dataset, and then used the best data augmentation policy obtained through training.

IV. EXPERIMENTS AND ANALYSIS

In this section, we comprehensively evaluate the improved YOLOv5 model through the TT100K [49, 50] dataset, which includes 182 types of traffic signs instances with detailed annotations and covers different actual traffic environments. And about 42.5% of traffic signs in TT100K are small objects, which means it is more suitable for actual vehicle-mounted target recognition. The size distribution of traffic sign instances in the dataset is displayed in Fig. 6.

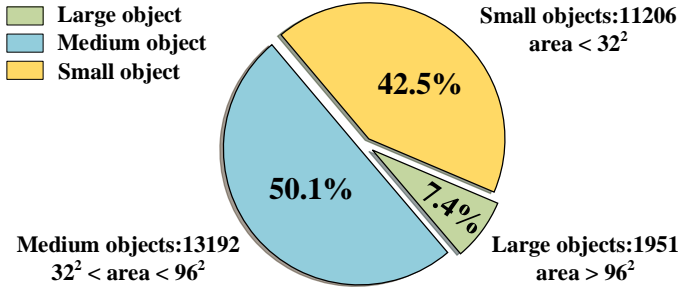


Fig. 6. Size distribution of sign instances from the TT100K.

A. Experimental setting

Considering the fixed size of input demanded by the

YOLOv5 network, we resized the images to uniform dimensions of 608×608. The training and validation datasets include 9146 images and the test dataset include 1121 image from TT100K. In the process of training, the initial value of the learning rate was 0.01, and use the cosine annealing strategy to reduce the learning rate. The epochs and the batch size are set to 500 and 32, respectively. Our experiments were performed on a Linux4.15.0-142-generic Ubuntu 18.04 with Intel(R) Xeon(R) Silver 4210R CPU @ 2.40GH, 8×32GB DDR4 and 8×TITAN Xp, 12GB memory. The mobile device used in the experiment is Jetson Xavier NX, and an external USB3.0 industrial camera.

B. Experimental analysis

To demonstrate the advantages of the proposed method in traffic sign detection, we evaluated our method on TT100K and compared it with the original YOLOv5, YOLOv5-Lite [51], EfficientDet [52], YOLOv5-face [53], M2det [54], SSD, and YOLOv3 [55]. We evaluated performance using metrics including model size, parameters, floating-point operations per second (FLOPs), mean average precision (mAP), average precision of large, medium, and small size targets (AP_L, AP_M, AP_S), and frames per second (FPS). The specific results are shown in Table I.

TABLE I

COMPARISON OF OUR METHOD WITH OTHER METHOD ON THE TT100K DATASET

Method	Model	Parameters	FLOPs	AP _S	AP _M	AP _L	mAP@0.5	FPS
Efficientdet-d0	15.15M	3.752M	2.50B	-	0.3980	0.5526	0.5786	26
M2det	340M	147M	16.35G	0.0300	0.3198	0.6586	0.4658	12
Mobilenet-SSD	118M	25.067M	29.20G	0.0275	0.2443	0.5261	0.3200	22
YOLOv3	119.6M	59.578M	158.00G	0.3889	0.4454	0.4288	0.6186	27
YOLOX-s	69.0M	9.010M	27.03G	0.4122	0.5975	0.6081	0.6860	59
YOLOv5-Lite-g	11.6M	5.277M	15.60G	0.3218	0.4914	0.4957	0.5431	71
YOLOv5	14.6M	7.193M	17.90G	0.3567	0.5142	0.5184	0.6018	105
Ours	16.3M	8.039M	17.90G	0.4146	0.5783	0.5817	0.6514	95

Firstly, it can be seen that the model size of the proposed method is 16.3M, which is easy to be deployed on a mobile platform so that it can be used for real-time shooting and recognition on the vehicle side. The amount of parameters in the training process is slight higher than that of Efficientdet and YOLOX. FLOPs is 17.9G, which is only 3.3G larger than the optimal YOLOv5-Lite. It can be seen from these two indicators that our method has a faster training speed and requires less hardware equipment, which is convenient for popularization. Excessive reduction of the number of parameters and calculations will lead to a decrease in the detection effect of the final training model. Secondly, our method achieves the mAP of 65.14% on all 182 traffic sign classes, which is second only to YOLOX. Although the AP_L of our method is lower than M2det and YOLOX, the recognition accuracy on small targets is 41.46%, which is significantly higher than other methods. Finally, FPS is used as a metric to evaluate the speed of target detection, indicating that our method can meet the real-time requirements of detection on the mobile terminal. In general, our method has high accuracy for multi-scale target detection, and can achieve a balance between recognition accuracy and recognition speed. The model size is suitable for deployment on the mobile terminal and has practical application significance.

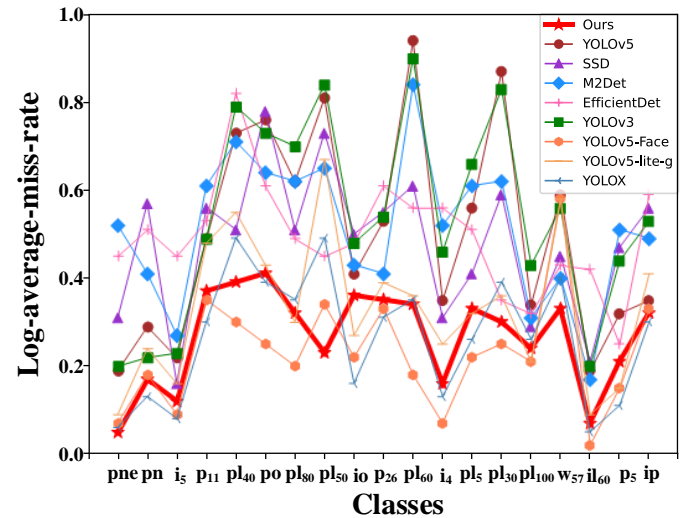


Fig. 7. Comparison of the miss detection rate of each method on 19 types of traffic signs.

In addition, traffic sign detection is a multi-category and multi-target recognition task, and the false detection rate and missed detection rate are also important metrics to measure the detection network. In order to verify the missed detection requirements of the proposed method in real-time traffic sign detection, Log-Average Miss RATE (LAMR) [56] is selected

as the evaluation index. LAMR reflects the relationship between the false negative (FP) of each image and the missed detection rate. The lower the FP, the better the detection performance of traffic signs. We selected the top 19 traffic sign categories in the dataset, and compared the missed detections of each method on these types of traffic signs, as shown in Fig. 7. It can be seen that the missed detection rate of our method for traffic sign recognition is significantly lower than other methods, and it has practical application significance. However, the missed detection rate of several types of traffic signs such as *ip*, *w57*, and *po* are still high, and we will make further improvements in future research.

We visualize the method proposed in this paper, as shown in Fig. 8(a). It can be observed that our method successfully recognized the small-sized traffic signs on the actual traffic scene with high recognition accuracy, and there are almost no missed detections and false detections. We transplanted the trained model to the mobile platform and connected an external camera to shoot the actual road scene. Real-time traffic sign detection and recognition are performed on the captured images, and the recognition results are displayed on the LED screen, as shown in Fig. 8(b).

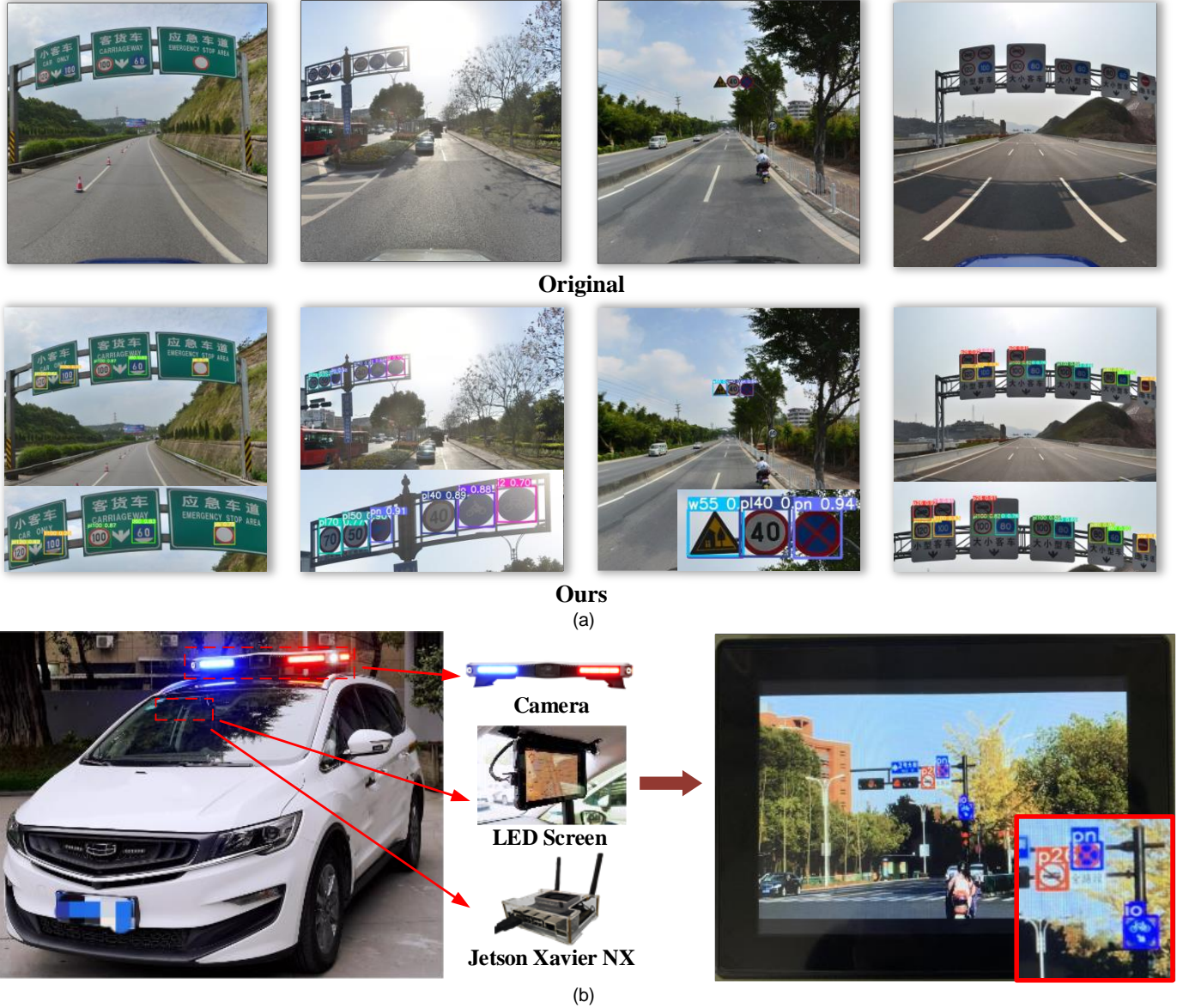


Fig. 8. (a). Some examples detected by our method on the TT100K dataset. (b) The mobile device deployment and the detection example of shooting through the camera.

C. Ablation Study

To more intuitively demonstrate the better performance of the proposed method for traffic sign detection and recognition, we conduct the ablation study, and the results are shown in Table II. It shows the ablation result of incrementally adding the components training on the YOLOv5s model.

TABLE II
ABLATION STUDY

Method	Model	Parameters	FLOPs	FPS	mAP
YOLOv5s	14.6M	7.193M	17.9G	105	0.6018
YOLOv5s+Aug	16.3M	7.193M	17.9G	105	0.6131
YOLOv5s+AF-FPN	14.6M	8.039M	17.9G	95	0.6267
Ours	16.3M	8.039M	17.9G	95	0.6514

As observed from the results, the standard YOLOv5s provides a detection mAP of 60.18%. Integrating the data augmentation and the AF-FPN improves the mAP to 61.31% and 62.67%, respectively. The mean average precision (mAP) of our method on the TT100K dataset is 4.96% higher than that of the YOLOv5s, which means the proposed method achieves impressive performance in target and recognition. At the same time, the model size and parameters amount only slightly increase, and the FLOPs do not change, which means that the training speed of the improved network and the requirements for training equipment are basically unchanged. These ensure that our method can be easily deployed on the vehicle side. Although FPS decreases by 10, it still meets the requirements of real-time detection on the vehicle side.

V. CONCLUSION

In this paper, we proposed a real-time traffic sign detection network based on modified YOLOv5s, which achieves better detection performance than state-of-art one-stage detectors. In this work, the proposed AF-FPN structure improves the information extraction ability of feature maps and its representation ability for detecting multi-scale objects. And the new data augmentation strategy enriches the traffic sign dataset by adding Noise, Mosaic and other methods to improve the training effect of the model. The empirical results verified that the proposed method could achieve state-of-the-art performance with a fast inference speed, the detection speed on the vehicle side is 95 FPS. The proposed method provides the input feature map of different receptive fields and fuses the receptive field pyramids for the target traffic signs. Therefore, the improved network can enhance the recognition accuracy of multi-scale targets without introducing additional calculations, the mAP has increased by 4.96% compared to the original network on the TT100K. Due to the size of the trained model being small, it is easy to deploy on the mobile device of the vehicle and perform real-time recognition and detection of the road scene. However, in practical applications, a faster vehicle speed will cause the motion blur of the image, which will affect the recognition result. In the future, we plan to explore a better performance detection model for high-speed moving targets.

REFERENCES

- [1] K. Z. Radu Timofte, Luc Van Gool, "Multi-view traffic sign detection, recognition, and 3D localisation," *2009 Workshop on Application of Computer Vision (WACV)*, 2009.
- [2] K. H. Shaoqing Ren, Ross Girshick, Jian Sun, "Faster R-CNN: Towards Real-Time Object Detection with Region Proposal Networks," *IEEE Transactions on Pattern Analysis and Machine Intelligence*, vol. 39, pp. 1137-1149, 2017.
- [3] Y. L. Jifeng Dai, Kaiming He, Jian Sun, "R-FCN: Object Detection via Region-based Fully Convolutional Networks," *30th Conference on Neural Information Processing Systems (NIPS 2016), Barcelona, Spain*, 2016.
- [4] W. Liu, D. Anguelov, D. Erhan *et al.*, "SSD: Single Shot MultiBox Detector," *Computer Vision – ECCV 2016. ECCV 2016. Lecture Notes in Computer Science*, vol. 9905, pp. 21-37, 2016.
- [5] J. Redmon, and A. Farhadi, "YOLO9000: Better, Faster, Stronger," *30th IEEE Conference on Computer Vision and Pattern Recognition (Cvpr 2017)*, pp. 6517-6525, 2017.
- [6] A. Pramanik, S. Sarkar, and J. Maiti, "A real-time video surveillance system for traffic pre-events detection," *Accident Analysis and Prevention*, vol. 154, May, 2021.
- [7] L. Shen, L. You, B. Peng *et al.*, "Group multi-scale attention pyramid network for traffic sign detection," *Neurocomputing*, vol. 452, pp. 1-14, 2021.
- [8] X. Z. Kaiming He, Shaoqing Ren, Jian Sun, "Deep residual learning for image recognition," *Computer Vision and Pattern Recognition*, pp. 770-778, 2016.
- [9] Ultralytics. "YOLOv5," <https://github.com/ultralytics/yolov5>.
- [10] E. D. Cubuk, B. Zoph, D. Mane *et al.*, "AutoAugment: Learning Augmentation Strategies from Data," *2019 IEEE/CVF Conference on Computer Vision and Pattern Recognition (Cvpr 2019)*, pp. 113-123, 2019.
- [11] X. Ning, K. Gong, W. Li *et al.*, "Feature Refinement and Filter Network for Person Re-identification," *IEEE Transactions on Circuits and Systems for Video Technology*, pp. 1-1, 2020.
- [12] X. Ning, P. F. Duan, W. J. Li *et al.*, "Real-Time 3D Face Alignment Using an Encoder-Decoder Network With an Efficient Deconvolution Layer," *IEEE Signal Processing Letters*, vol. 27, pp. 1944-1948, 2020.
- [13] C.-Y. W. Alexey Bochkovskiy, Hong-Yuan Mark Liao, "Yolov4: Optimal Speed and Accuracy of Object Detection," *Computer Vision and Pattern Recognition*, 2020.
- [14] W. L. Ouyang, X. G. Wang, X. Y. Zeng *et al.*, "DeepID-Net: Deformable Deep Convolutional Neural Networks for Object Detection," *2015 IEEE Conference on Computer Vision and Pattern Recognition (Cvpr)*, pp. 2403-2412, 2015.
- [15] F. M. Shao, X. Q. Wang, F. J. Meng *et al.*, "Real-Time Traffic Sign Detection and Recognition Method Based on Simplified Gabor Wavelets and CNNs," *Sensors*, vol. 18, no. 10, Oct, 2018.
- [16] F. M. Shao, X. Q. Wang, F. J. Meng *et al.*, "Improved Faster R-CNN Traffic Sign Detection Based on a Second Region of Interest and Highly Possible Regions Proposal Network," *Sensors*, vol. 19, no. 10, May 2, 2019.
- [17] J. Zhang, M. Huang, X. Jin *et al.*, "A Real-Time Chinese Traffic Sign Detection Algorithm Based on Modified YOLOv2," *Algorithms*, vol. 10, no. 4, 2017.
- [18] J. A. Li, X. D. Liang, Y. Wei *et al.*, "Perceptual Generative Adversarial Networks for Small Object Detection," *30th IEEE Conference on Computer Vision and Pattern Recognition (Cvpr 2017)*, pp. 1951-1959, 2017.
- [19] Z. W. Liu, C. Shen, M. Y. Qi *et al.*, "SADANet: Integrating Scale-Aware and Domain Adaptive for Traffic Sign Detection," *IEEE Access*, vol. 8, pp. 77920-77933, 2020.
- [20] L. S. D. Bharat Singh, "An Analysis of Scale Invariance in Object Detection - SNIP," *arXiv:1711.08189 [cs.CV]*, 2018.
- [21] Y. L. Yukang Chen, Tao Kong, Lu Qi, Ruihang Chu, Lei Li, Jiaya Jia, "Scale-aware Automatic Augmentation for Object Detection," *arXiv:2103.17220*, 2021.
- [22] J.-q. Luo, H.-s. Fang, F.-m. Shao *et al.*, "Multi-scale traffic vehicle detection based on faster R-CNN with NAS optimization and feature enrichment," *Defence Technology*, 2020.
- [23] T. Y. Lin, P. Dollar, R. Girshick *et al.*, "Feature Pyramid Networks for Object Detection," *30th IEEE Conference on Computer Vision and Pattern Recognition (Cvpr 2017)*, pp. 936-944, 2017.
- [24] K. M. He, G. Gkioxari, P. Dollar *et al.*, "Mask R-CNN," *2017 IEEE International Conference on Computer Vision (Iccv)*, pp. 2980-2988, 2017.
- [25] T. Y. Lin, P. Goyal, R. Girshick *et al.*, "Focal Loss for Dense Object Detection," *2017 IEEE International Conference on Computer Vision (Iccv)*, pp. 2999-3007, 2017.
- [26] Y. X. Leilei Cao, Lin Xu, "EMface Detecting Hard Faces by Exploring Receptive Field Pyramids," *Computer Vision and Pattern Recognition*, 2021.
- [27] J. Deng, W. Dong, R. Socher *et al.*, "ImageNet: A Large-Scale Hierarchical Image Database," *Cvpr: 2009 IEEE Conference on Computer Vision and Pattern Recognition, Vols 1-4*, pp. 248-255, 2009.
- [28] A. Z. Karen Simonyan, "Very deep convolutional networks for large-scale image recognition," *CoRR*, 2014.
- [29] C. Shorten, and T. M. Khoshgoftaar, "A survey on Image Data Augmentation for Deep Learning," *Journal of Big Data*, vol. 6, no. 1, 2019.
- [30] L. Taylor, and G. Nitschke, "Improving Deep Learning with Generic Data Augmentation," *2018 IEEE Symposium Series on Computational Intelligence (Ieee Ssci)*, pp. 1542-1547, 2018.
- [31] H. Zhang, and Q. M. J. Wu, "Pattern Recognition by Affine Legendre Moment Invariants," *2011 18th IEEE International Conference on Image Processing (Icip)*, pp. 797-800, 2011.

- [32] J. J. Lv, C. Cheng, G. D. Tian *et al.*, "Landmark perturbation-based data augmentation for unconstrained face recognition," *Signal Processing-Image Communication*, vol. 47, pp. 465-475, Sep, 2016.
- [33] G. E. H. Vinod Nair, "Rectified linear units improve restricted boltzmann machines," *International Conference on International Conference on Machine Learning. Omnipress*, 2010.
- [34] D. Dwibedi, I. Misra, and M. Hebert, "Cut, Paste and Learn: Surprisingly Easy Synthesis for Instance Detection," *2017 IEEE International Conference on Computer Vision (ICCV)*, pp. 1310-1319, 2017.
- [35] J. S. Hao-Shu Fang, Runzhong Wang, Minghao Gou, Yong-Lu Li, Cewu Lu, "InstaBoost: Boosting Instance Segmentation via Probability Map Guided Copy-Pasting," *arXiv:1908.07801 [cs.CV]*, 2019.
- [36] B. Singh, M. Najibi, and L. S. Davis, "SNIPER: Efficient Multi-Scale Training," *Advances in Neural Information Processing Systems 31 (NIPS 2018)*, vol. 31, 2018.
- [37] T. Tran, T. Pham, G. Carneiro *et al.*, "A Bayesian Data Augmentation Approach for Learning Deep Models," *Advances in Neural Information Processing Systems 30 (NIPS 2017)*, vol. 30, 2017.
- [38] X. Shi, J. Hu, X. Lei *et al.*, "Detection of Flying Birds in Airport Monitoring Based on Improved YOLOv5," in *2021 6th International Conference on Intelligent Computing and Signal Processing (ICSP)*, 2021, pp. 1446-1451.
- [39] S. Liu, L. Qi, H. Qin *et al.*, "Path Aggregation Network for Instance Segmentation," in *2018 IEEE/CVF Conference on Computer Vision and Pattern Recognition*, 2018, pp. 8759-8768.
- [40] H. Rezatofighi, N. Tsoi, J. Gwak *et al.*, "Generalized Intersection over Union: A Metric and A Loss for Bounding Box Regression," *2019 IEEE/CVF Conference on Computer Vision and Pattern Recognition (CVPR 2019)*, pp. 658-666, 2019.
- [41] Y. H. He, C. C. Zhu, J. R. Wang *et al.*, "Bounding Box Regression with Uncertainty for Accurate Object Detection," *2019 IEEE/CVF Conference on Computer Vision and Pattern Recognition (CVPR 2019)*, pp. 2883-2892, 2019.
- [42] P. W. W. L. zhaohui Zheng, Jinze Li, Rongguang Ye, Dongwei Ren, "Distance-IoU Loss: Faster and Better Learning for Bounding Box Regression," *AAAI Conference on Artificial Intelligence*, 2020.
- [43] M. Kim, C. Park, S. Kim *et al.*, "Efficient Dilated-Winograd Convolutional Neural Networks," *2019 IEEE International Conference on Image Processing (ICIP)*, pp. 2711-2715, 2019.
- [44] K. M. He, X. Y. Zhang, S. Q. Ren *et al.*, "Spatial Pyramid Pooling in Deep Convolutional Networks for Visual Recognition," *IEEE Transactions on Pattern Analysis and Machine Intelligence*, vol. 37, no. 9, pp. 1904-1916, Sep, 2015.
- [45] E. D. C. Baeert Zoph, Golnaz Ghiasi, Tsung-Yi Lin, Jonathon Shlens, Quoc V. Le, "Learning Data Augmentation Strategies for Object Detection," *arXiv:1906.11172 [cs.CV]*, 2019.
- [46] X. W. Shaoli Huang, Dacheng Tao, "SnapMix: Semantically Proportional Mixing for Augmenting Fine-grained Data," 2020.
- [47] Z. Wang, H. Li, Z. X. Wu *et al.*, "A pretrained proximal policy optimization algorithm with reward shaping for aircraft guidance to a moving destination in three-dimensional continuous space," *International Journal of Advanced Robotic Systems*, vol. 18, no. 1, Jan, 2021.
- [48] B. Zoph, V. Vasudevan, J. Shlens *et al.*, "Learning Transferable Architectures for Scalable Image Recognition," *2018 IEEE/CVF Conference on Computer Vision and Pattern Recognition (CVPR)*, pp. 8697-8710, 2018.
- [49] Y. Zhu, C. Zhang, D. Zhou *et al.*, "Traffic sign detection and recognition using fully convolutional network guided proposals," *Neurocomputing*, vol. 214, pp. 758-766, 2016.
- [50] Z. Zhu, D. Liang, S. H. Zhang *et al.*, "Traffic-Sign Detection and Classification in the Wild," *2016 IEEE Conference on Computer Vision and Pattern Recognition (CVPR)*, pp. 2110-2118, 2016.
- [51] "YOLOv5-Lite," <https://github.com/ppogg/YOLOv5-Lite>.
- [52] R. P. M. Tan, Q. V. Le, "EfficientDet: Scalable and Efficient Object Detection," *Proceedings of the IEEE/CVF Conference on Computer Vision and Pattern Recognition*, pp. 10781-10790, 2020.
- [53] W. T. Delong Qi, Qi Yao, Jingfeng Liu, "YOLO5Face: Why Reinventing a Face Detector," 2021.
- [54] T. S. Q. Zhang, Y. Wang, Z. Tang, Y. Chen, L. Cai, H. Ling, "M2Det A Single-Shot Object Detector based on Multi-Level Feature Pyramid Network," *Proceedings of the AAAI Conference on Artificial Intelligence*, vol. 33, pp. 9259-9266, 2019.
- [55] A. F. J. Redmon, "YOLOv3: An Incremental Improvement," *arXiv preprint arXiv:1804.02767*, 2018.

- [56] P. Dollar, C. Wojek, B. Schiele *et al.*, "Pedestrian Detection: An Evaluation of the State of the Art," *IEEE Transactions on Pattern Analysis and Machine Intelligence*, vol. 34, no. 4, pp. 743-761, Apr, 2012.



Junfan Wang received the B.E. degree in Electronic Information Science and Technology from Wenzhou University, Wenzhou, Zhejiang, in 2020. She is currently working toward the master's degree in Electronic Science and Technology at the Hangzhou Dianzi University. Her research interests cover artificial neural network and vehicle-road synergy



Yi Chen received the B.E. degree in Hangzhou Dianzi University Information Engineering School in 2016. He is studying for a M.E. degree at Hangzhou University of Electronic Science and Technology. His research interests are in the area of Computer Vision.



Mingyu Gao was born in 1963. He received the M.S. degree in power electronics from Zhejiang University, Hangzhou, China, in 1993, and the Ph.D. degree in information and communication engineering from the Wuhan University of Technology, Wuhan, China, in 2013.

In 2001, he joined Hangzhou Dianzi University, Hangzhou, China, where he is currently a Professor with the School of Electronic and Information. His research

interests include electronics and vehicle electronics.



Zhekang Dong received the B.E. and M.E. degrees in electronics and information engineering in 2012 and 2015, respectively, from Southwest University, Chongqing, China. He received the Ph.D. degree from the School of Electrical Engineering, Zhejiang University, China, in 2019. Currently, he is an associate professor in Hangzhou Dianzi University, Hangzhou, China. He is also a Research Assistant (Joint-Supervision) at The Hong Kong Polytechnic University. His research interests cover memristor and memristive system, artificial neural network, the design

and analysis of nonlinear systems based on memristor and computer simulation.